Cs$_2$ 'diffuse bands' emission from superheated cesium vapor

Cs₂ 'diffuse bands' emission from superheated cesium vapor

G Pichler[1], Y Makdisi[1], J Kokaj[1], N Thomas[1], J Mathew[1] and R Beuc[2]

[1] Physics Department, Kuwait University, PO Box 5969, 13060—Safat, Kuwait
[2] Institute of Physics, HR-10000 Zagreb, Croatia

E-mail: pichler@ifs.hr

CrossMark

Abstract
Thermal emission from superheated cesium vapor was studied to very high temperatures from 700 °C to 1000 °C. This was performed in the vapor condition only and with no liquid cesium present in the all-sapphire cell. We observed a number of atomic and molecular spectral features simultaneously in emission and absorption, especially peculiar thermal emission of cesium dimer diffuse bands ($2\,^3\Pi_g \rightarrow a\,^3\sum_u^+$ transitions) around 710 nm coexisting with absorption bands around first resonance lines at 852 and 894 nm. We performed appropriate calculations of the diffuse band emission profiles and compared them with measured profiles. We also performed absorption measurements and compared observed diffuse band profiles with calculated ones. Possible applications of the observed phenomena will be discussed in terms of the solar energy conversion using dense cesium vapor.

Keywords: emission and absorption spectroscopy, superheated cesium vapor, cesium diffuse bands

(Some figures may appear in colour only in the online journal)

1. Introduction

Superheating in alkali cells leads to thermal destruction of the alkali molecules, which have been used in the past for several purposes. It was used for the determination of the atomic number density in dense Cs vapors by absorption measurements of Cs₂ triplet bands, where the overheated cesium vapor was generated in a heat pipe oven [1]. Furthermore it was employed in the study of the overheated potassium molecules [2]. Superheating of cesium vapor was applied in order to recognize triplet transitions from singlet transitions in the Cs₂ molecule [3]. In the study of the conical emission from dense cesium vapor, superheating was decisive in arriving at the conclusion that the nonlinear formation process is connected to Cs₂ molecules [4].

One of the main purposes in many experiments was to get rid of the molecular contribution in the spectrum and to observe pure atomic spectral phenomena. Recently, superheating with effective thermal destruction of molecules was used to study structured photoionization continuum of the cesium vapor [5] in which both atomic and molecular contributions were present at diverse fractions at different temperatures. From the molecular destruction behavior, at superheated conditions, it was possible to extract the pure molecular contribution to the photoionization process of Cs₂.

Here we performed two experiments with hot cesium vapor in an all-sapphire cell. In one we measured the absorption coefficient by using a background light source and in another using self emission from the oven with the cesium cell at temperatures between 700 °C and 1000 °C, where superheating conditions exist. In the thermal emission experiment we found peculiar emission of cesium dimer diffuse bands around 710 nm. In addition, we calculated the reduced absorption coefficient (k/N^2, where k is absorption coefficient and N the cesium atom density) for temperatures from 700 to 1400 K in order to identify small differences in shapes and size of the diffuse band components at 705, 707, 713 and 719 nm, which can eventually be used for diagnostic purposes at high temperature and densities of the cesium thermionic devices. It should be noted that the Cs atom density remains essentially the same in the above-mentioned temperature interval [6].

Even when cesium dimers (in singlet ground state) are greatly reduced at very high temperatures, cesium diffuse

J. Phys. B: At. Mol. Opt. Phys. **49** (2016) 145101

G Pichler *et al*
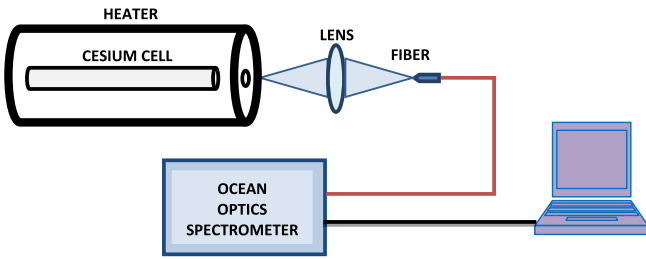
Figure 1. Experimental setup.

bands (triplet state manifold) peaking at 705, 707, 713 and 719 nm can be observed both in the absorption and the emission spectrum. This is because they emerge from the triplet potential curves manifold, which is an excimer system [7, 8]. This is also valid for the molecular bands located under the forbidden lines of cesium peaking at 684.9 nm and 689.5 nm [9].

2. Experiment

A cesium all-sapphire cell of 16 cm in length was heated within a cylindrical oven. The temperature of the cell was measured using a thermocouple positioned at the end side of the cell. The cell was completely enclosed and isolated except for two small openings for collection of emitted light and light transmission measurements. An all-sapphire cell containing a very small droplet of cesium [5] was heated to temperatures up to 1000 °C (figure 1). The emission spectrum from the cell was acquired using an OceanOptics spectrometer (HR4000CG-UV-NIR) with QP600-2-VIS-NIR fiber. The cell was heated slowly from room temperature up to 700 °C where it was held for about one hour in order to make measurements at equilibrium conditions. The temperature was then increased and held constant for one hour in order to accomplish the measurement. This was repeated until a final temperature of 1000 °C. We observed a red glow from the oven at 700 °C. But at higher temperatures we clearly observed characteristic Cs_2 molecular bands and Cs atomic spectral lines in emission and absorption.

In order to determine the absorption coefficient of the cesium superheated vapor in the temperature range from 700 °C to 1000 °C we performed transmission measurements using a laser driven light source (LDLS, Model EQ-99-FC, Energetiq [10]) as a background continuum. The relevant experimental setup is similar to figure 1 except that the laser induced xenon plasma (LDLS) light beam was fed into the appropriate fiber from which the light was transmitted through the hot and superheated cesium vapor. The OceanOptics spectrometer was again used to display the transmission spectrum on the laboratory laptop and the absorption coefficient was deduced by using the Beer–Lambert law, $k = \frac{1}{L} \ln \frac{I_o}{I}$, where k is an absorption coefficient, L the length of the cell, I_o the intensity at the entrance of the cell, and I is the transmitted intensity through the cell.
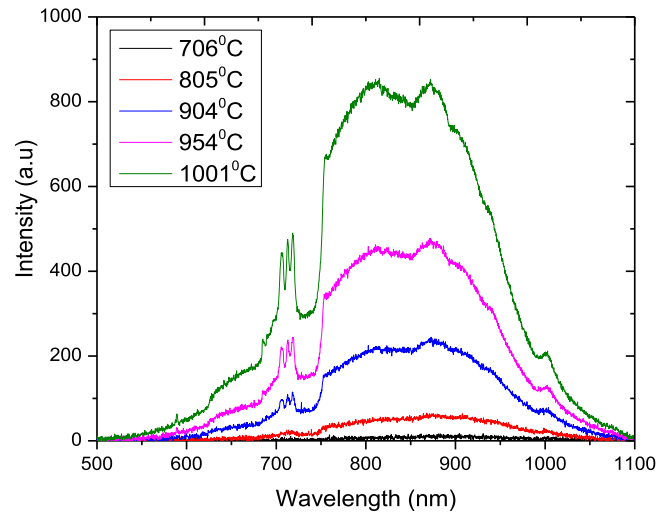
Figure 2. Thermal emission from the superheated cesium vapor at five different temperatures, without correction for the spectral sensitivity. Each spectrum was averaged 10 times.

In our all-sapphire cell the amount of liquid cesium was so small that at a temperature of about 420 °C all the liquid cesium evaporated. This can be described as a critical temperature, T_c. Atomic densities, $N(Cs) = 3.4 \times 10^{17} \, cm^{-3}$, according to the empiric formula given by Taylor and Langmuir [11], will remain the same, while the molecular densities of $N(Cs_2) = 8 \times 10^{15} \, cm^{-3}$, according to Nesmeyanov [12], will steadily decrease above this critical temperature T_c. This means that at higher temperature the molecular density will decrease due to increasingly effective thermal collisions leading to dimer destruction. The molecular fraction to the total density at this critical temperature is a bit more than about 2%. The transition from the saturated vapor at T_c into the superheated vapor will cause the lowering of cesium dimer density. In reference [13] the authors had two all-sapphire cells with different cesium droplet fillings and they observed a lower critical temperature when the droplet of cesium was smaller. In the temperature range of our experiment cesium vapor was superheated, which means that the fraction of Cs_2 molecules decreased from a few percent at 420 °C toward extremely small value at 1000 °C.

3. Results

3.1. Experimental results

In figure 2 we present thermal emission from the superheated cesium vapor at five different temperatures. The measured spectrum was not corrected for the spectral sensitivity. At the lowest temperature of 706 °C (979 K) we cannot discern any structure in the very weak continuum emission which just started to exhibit a red glow from the cesium vapor. However, at 805 °C (1078 K) the structure above 700 nm just appeared, and then at temperatures of 904 °C (1177 K), 954 °C (1227 K) and 1001 °C (1274 K) we definitely observed nicely developed diffuse bands in emission, peaking at 705, 707, 713 and
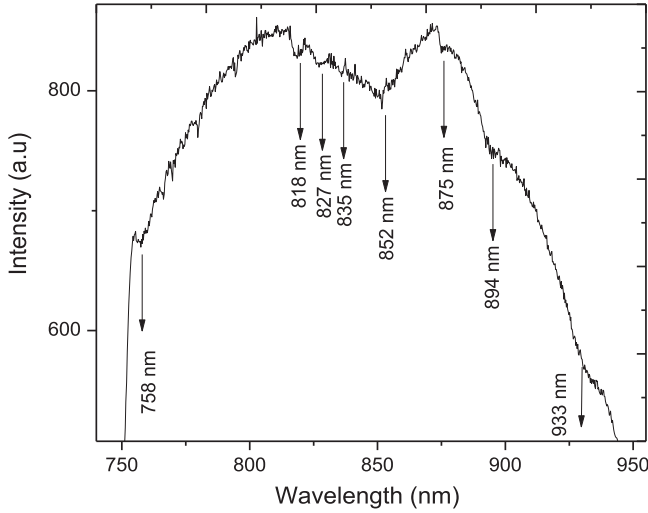
Figure 3. Enlarged portion between 750 and 950 nm with several Cs and Cs$_2$ absorption features at 1001 °C.
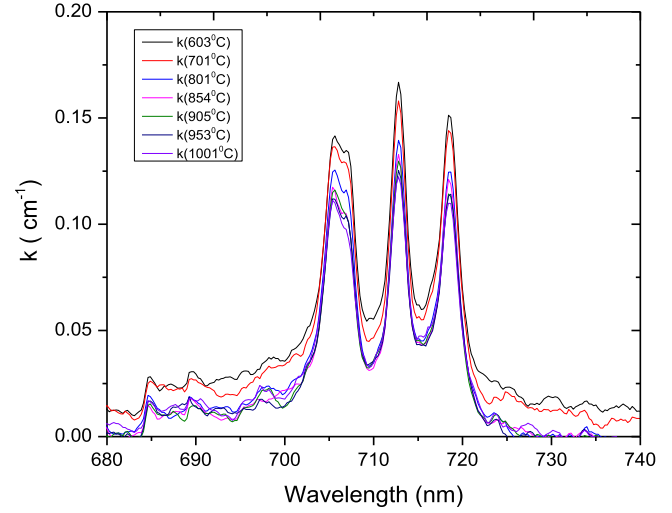
Figure 5. Absorption spectrum of the diffuse bands at different temperatures.
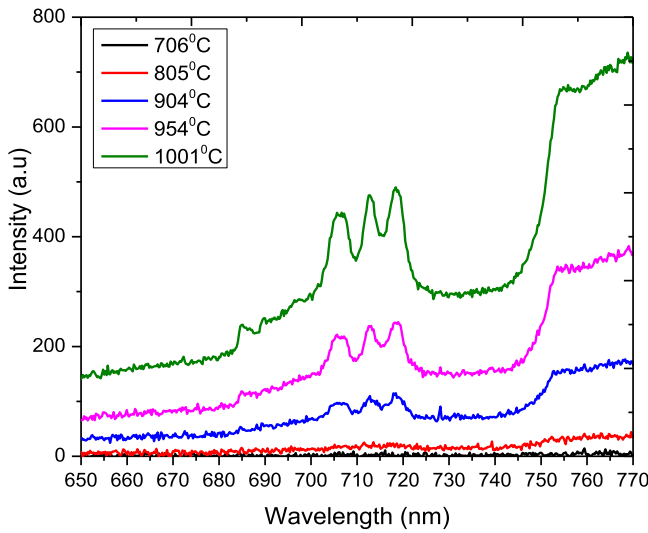
Figure 4. Cs$_2$ diffuse bands together with self-broadened Cs forbidden lines observed in emission.

719 nm [7]. At the highest temperature of 1001 °C (maximum of the corresponding black body function lies at 2.35 μm), we also saw Cs forbidden lines in emission peaking at 684.9 and 689.5 nm. Merged resonance lines of sodium at 589.0/0.6 nm also appeared in emission.

In figure 3 we present an enlarged portion from 750 nm up to 950 nm, where we can see absorption of the Cs D2 852 nm and Cs D1 894 nm resonance lines, with accompanying satellite bands, also in absorption, at 818, 827, 835 and 875 nm [14, 15]. At 933 and 992 nm there are absorption dips corresponding to the optical fiber attenuation bands.

In figure 4 we present the emission between 650 and 760 nm, where Cs$_2$ diffuse bands and adjacent forbidden lines are shown at various oven temperatures. We note the profound hole between 725 and 750 nm. At 758 nm we may observe the small dip corresponding to the peak of the Cs$_2$ B ← X absorption band. We assume that between 725 and 760 nm there is almost negligible emission of the blue edge of

the Cs$_2$ B → X band. Cs$_2$ diffuse bands do not contribute at wavelengths longer than 725 nm. We also performed transmission measurements in order to obtain the relevant absorption spectra at similar temperatures as in the emission experiment. The results are shown in figure 5.

3.2. Theoretical results

Three groups of optical transitions contribute to the emission and absorption in the spectral region between 680 and 740 nm; two triplet transitions $2^3\Pi_g(2_g, 1_g, 0_g^\pm) \rightarrow a^3\Sigma_u^+(1_u, 0_u^-)$, $2^3\Sigma_g^+(2_g, 1_g, 0_g^\pm) \rightarrow a^3\Sigma_u^+(1_u, 0_u^-)$ and one singlet transition $2^1\Sigma_u^+(0_u^+) \rightarrow X^1\Sigma_g^+(0_g^+)$. Ground electronic singlet $X^1\Sigma_g^+(0_g^+)$ and triplet $a^3\Sigma_u^+(1_u, 0_u^-)$ states have a common asymptote Cs$6S_{\frac{1}{2}}$ + Cs$6S_{\frac{1}{2}}$, whereas excited singlet $2^1\Sigma_u^+(0_u^+)$ and triplet $2^3\Pi_g(2_g, 1_g, 0_g^\pm)$, $2^3\Sigma_g^+(2_g, 1_g, 0_g^\pm)$ electronic states have the same asymptote at Cs$6S_{\frac{1}{2}}$ + Cs$5D_{\frac{3}{2},\frac{5}{2}}$. Potential curves of these electronic states given by Spies [16] are shown in figure 6(a). Difference potential curves for the relevant transitions are shown on figure 6(b). All difference potentials of triplet $2^3\Pi_g(2_g, 1_g, 0_g^\pm) \rightarrow a^3\Sigma_u^+(1_u, 0_u^-)$ transitions have two extrema (minima and maxima). Difference potentials of $2^3\Sigma_g^+(2_g, 1_g, 0_g^\pm) \rightarrow a^3\Sigma_u^+(1_u, 0_u^-)$ are monotonic in the region of interest, and the difference potential of $2^1\Sigma_u^+(0_u^+) \rightarrow X^1\Sigma_g^+(0_g^+)$ transition has one minimum very close to minima of the $2^3\Pi_g(2_g) \rightarrow a^3\Sigma_u^+(1_u)$ transition. In the region of interest, there is no important mixing of $2^1\Sigma_u^+(0_u^+)$, $2^3\Sigma_g^+(1_g, 0_g^+)$ and $2^3\Pi_g(2_g, 1_g, 0_g^\pm)$ with other states due to spin–orbit interaction. Energies of components of $2^3\Sigma_g^+(1_g, 0_g^+)$ are almost degenerate $E_{2^3\Sigma_g^+}(R) \approx E_{1_g}(R) \approx E_{0_g^+}(R)$, where $E_{2^3\Sigma_g^+}(R)$ is energy of the $2^3\Sigma_g^+$ state in Hund's case (a). The energies of $2^3\Pi_g$ state components can be roughly described as a Hund's case (a) energy of $2^3\Pi_g$ state split by spin–orbit interaction $E_{\Omega_g^{(\pm)}}(R) = E_{2^3\Pi_g}(R) + (\Omega - 1)\Delta_{so}(R)/3$, where $\Delta_{so}(R)$
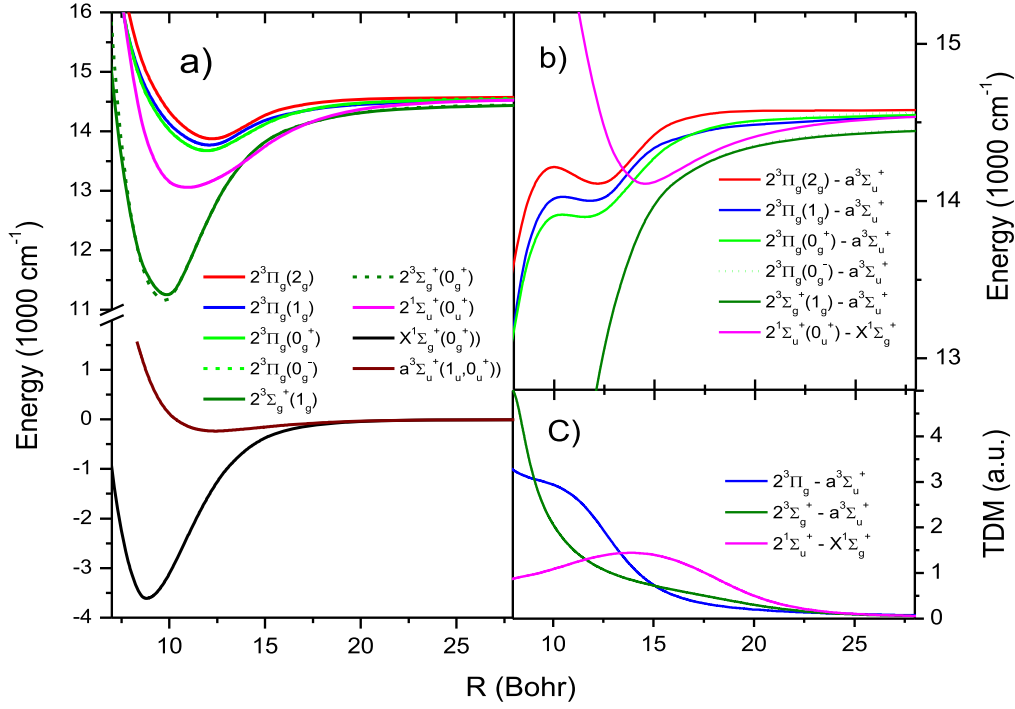
Figure 6. (a) Cs_2 potential curves of electronic states: $2^3\Pi_g(2_g, 1_g 0_g^\pm)$, $2^3\Sigma_g^+(2_g, 1_g 0_g^\pm)$, $2^1\Sigma_u^+(0_g^+)$, $a^3\Sigma_u^+(1_u 0_g^-)$ and $X^1\Sigma_g^+(0_g^+)$ [16], (b) difference potential curves for relevant transitions contributing in the 685–740 nm spectral range, (c) corresponding transition dipole moments (TDMs) [17].

have a meaning of the spin–orbit interaction in $2^3\Pi_g$ state. These where the plausible reasons for approximations of transition dipole moments (TDMs) $D_{\alpha' \to \alpha''}(R)$, ($\alpha''$ and α' label the lower and the upper electronic molecular state, respectively) $D_{2^3\Pi_g(\Omega_g') \to a^3\Sigma_u^+(\Omega_u'')}(R) = D_{2^3\Pi_g \to a^3\Sigma_u^+}(R)$, $D_{2^3\Sigma_g^+(\Omega_u') \to a^3\Sigma_u^+(\Omega_u'')}(R) = D_{2^3\Sigma_g^+ \to a^3\Sigma_u^+}(R)$ and $D_{2^1\Sigma_u^+(\Omega_u') \to X^1\Sigma_g^+(\Omega_g'')}(R) = D_{2^1\Sigma_u^+ \to X^1\Sigma_g^+}(R)$ where $\Omega = 0^\pm, 1, 2$.

At temperature T and frequency of the absorbed photon ν, the thermally averaged reduced absorption coefficient $k_{\alpha'',\alpha'}(\nu, T)$ for the transition between two electronic states of a diatomic molecule, using semi-quantum approximation, can be written as [17]:

$$k_{\alpha'',\alpha'}(\nu, T) = W \frac{16\pi^3\sqrt{2\pi}}{c\sqrt{\mu k_B T}} \nu \sum_{v'',v'} \exp\left(-\frac{E_{v'',0,\varepsilon''}}{k_B T}\right)$$
$$\times |\langle \Phi_{v'',0,\alpha''} |RD_{\alpha' \to \alpha''}(R)| \Phi_{v',0,\alpha'}\rangle|^2 g(\nu - \nu_{tr}): \quad (1)$$

where v is the vibrational quantum number, $\Phi_{v,0,\alpha}$ and $E_{v,0,\alpha}$ are the radial wave function and energy of state with rotational quantum number $J = 0$. μ is molecule reduced mass. W is statistical factor $W = \frac{1}{12}$ for a transition where in an upper state $\Omega' = 1, 2$, and $W = \frac{1}{24}$ for $\Omega' = 0$. Function $g(\nu - \nu_{tr})$ simulates the instrumental profile of the spectrometer, where the transition energy is given by $h\nu_{tr} = E_{v',0,\alpha'} - E_{v'',0,\alpha''}$. We collected transitions in bins of the size $\Delta\nu/c = 2\,\text{cm}^{-1}$, and smoothed with triangle profile with FWHM $10\,\text{cm}^{-1}$. So in our synthetic spectra the function $g(\nu - \nu_{tr})$ has a meaning of low resolution instrumental profile.

Using the Fourier-grid Hamiltonian method [18], where vibrational wave functions are represented on a finite number of uniformly spaced grid points R_i, the energies $E_{v,0,\alpha}$ and the wave functions $\Phi_{v,0,\alpha}$ are obtained by a diagonalization of the Hamiltonian matrix H:

$$H_{i,j} = \frac{\hbar^2}{2\mu\Delta R^2} \left\{ \begin{array}{ll} \dfrac{\pi^2}{3} - \dfrac{1}{2i^2} & i = j \\ (-1)^{i-j}\dfrac{8ij}{(i^2-j^2)^2} & i \neq j \end{array} \right\}$$
$$+ \left[V_\alpha(R_i) + \frac{\hbar^2}{2\mu}\frac{\Omega^2}{R_i^2}\right]\delta_{i,j}, \quad (2)$$

where $V_\alpha(R)$ is the adiabatic potential of electronic state, Ω is electronic angular moment of this state, and ΔR is the distance between two grid points.

The thermal emission from a uniform layer of thickness L and atomic number density N is related to the reduced absorption coefficient $k(\nu, T)$ by Kirchhoff's law of thermal radiation [19–21]. Spectral radiance $I(\nu, T)$ (in units of erg s^{-1} Sr^{-1} cm^{-2} Hz^{-1}) can be written as:

$$I(\nu, T) = \frac{2h\nu^3}{c^2}\frac{1}{e^{h\nu/k_B T} - 1}$$
$$\times \{1 - e^{-N^2 L k(\nu,T)[1-\exp(-h\nu/k_B T)]}\} \quad (3)$$

Using the potential curves of electronic states and the corresponding transition dipole moments [17], we calculated absorption and emission spectra for the set of experimental temperatures. On figure 7 are contributions to the reduced

J. Phys. B: At. Mol. Opt. Phys. **49** (2016) 145101

G Pichler *et al*
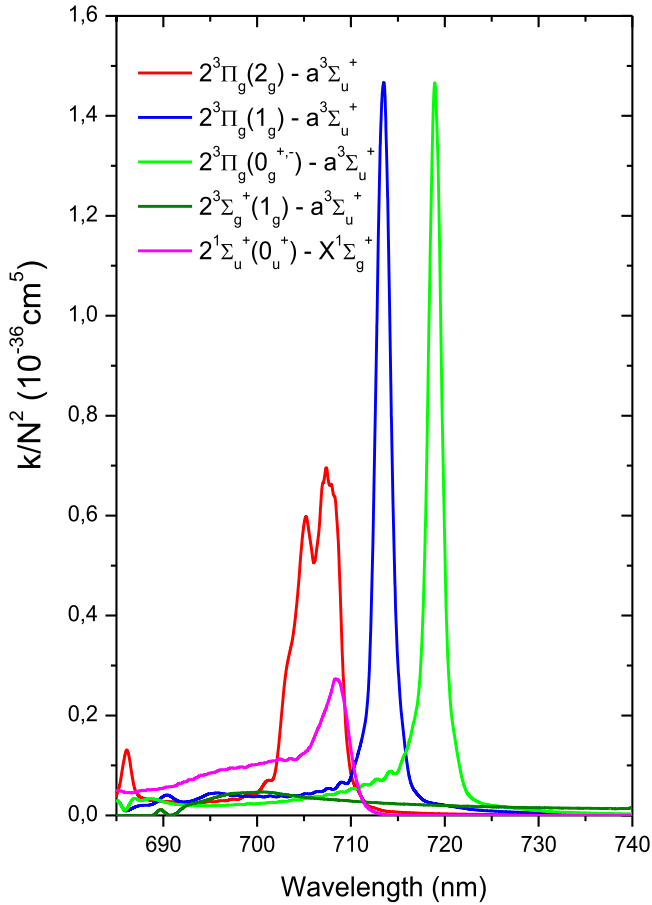
Figure 7. Calculated contributions to the reduced absorption coefficient in the spectral region of the diffuse bands.

Figure 8. Comparison of experimental and theoretical reduced absorption coefficient within the Cs_2 diffuse bands at five different temperatures of the sapphire cell.

absorption coefficient of each electronic transition, calculated at temperature 1001 C. Absorption spectra of $2^3\Pi_g(2_g) \rightarrow a^3\Sigma_u^+(1_u, 0_u^-)$ have two maxima at 705.2 and 707.2 nm which correspond to the maxima and minima in the difference potential curve. $2^3\Pi_g(1_g) \rightarrow a^3\Sigma_u^+(1_u, 0_u^-)$ transition contribution has one extremum at 713.6 nm corresponding to close spaced maxima and minima in difference potential. Similarly, $2^3\Pi_g(0_g^\pm) \rightarrow a^3\Sigma_u^+(1_u, 0_u^-)$ transition spectrum has an extremum at 719.0 nm. Singlet $2^1\Sigma_u^+(0_u^+) \rightarrow X^1\Sigma_g^+(0_g^+)$ transition spectrum has maximum at 708.4 nm corresponding to the minimum in the difference potential. Triplet $2^3\Sigma_g^+(2_g, 1_g, 0_g^\pm) \rightarrow a^3\Sigma_u^+(1_u, 0_u^-)$ transition gives a small and monotonic contribution in the spectral region of interest. All these contribution come from the region of weakly attractive electronic $X^1\Sigma_g^+(0_g^+)$ and $a^3\Sigma_u^+(1_u, 0_u^-)$ ground states, so the absorption coefficient is not very sensitive on temperature changes.

4. Discussion

The measured absorption coefficient from figure 5, when divided by the critical cesium atom density at 420 °C is now shown in figure 8(a) as a reduced absorption coefficient. In figure 8(b) we present theoretically calculated reduced

absorption coefficient. The comparison is relatively good and shows that the peak absorption at 705, 707, 713 and 719 nm is between 1×10^{-36} and 1.5×10^{-36} cm^5. This means that the emission profiles at 705, 707, 713 and 719 nm will be slightly self-absorbed, especially at band centers. Previous absorption measurements by Vadla *et al* [1] show similar values of the reduced absorption coefficients in somewhat smaller wavelength region which included Cs_2 diffuse bands. From our previous measurements we know that the absorption coefficient in the spectral region above 750 nm is much larger than 1 cm^{-1} indicating that all spectral features at longer wavelength than 750 nm will appear in observed oven emission spectrum as slightly absorbed spectral features. This may be seen in figure 3.

The experimentally observed emission of the Cs_2 diffuse bands as shown in figure 4 is now reproduced in figure 9(a). In figure 9(b) we present theoretically calculated emission coefficient of the Cs_2 diffuse bands in the spectral region between 685 and 740 nm, for the same temperatures. It may be seen that the highest temperature reveals the largest emission of the diffuse bands both theoretically and experimentally.

The theoretical calculation of the emission of the Cs_2 diffuse bands peaking at 705.2, 707.2, 713.6 and 719 nm as shown in figure 9(b) are narrower than experimentally
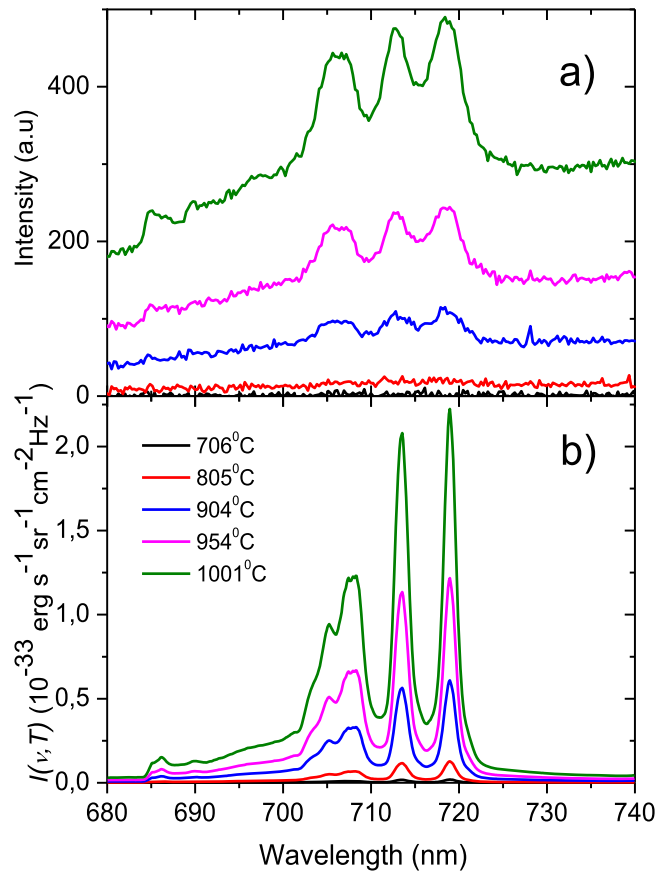
Figure 9. (a) Experimentally observed emission of the Cs_2 diffuse bands, (b) theoretically calculated emission coefficient of the Cs_2 diffuse bands, in the spectral region between 680 and 740 nm, for five temperatures.

observed as shown in figure 9(a). This is due to the small absorption coefficient around the core of these bands, as mentioned above. If the initial cesium filling would be smaller than in the present case, then the smaller amount of cesium atom density will be present in the superheated condition and the emission at diffuse bands would occur in more optically thin case. Consequently, the comparison between observed and calculated diffuse band profiles would have much better agreement, as expected.

Since the largest emission of the diffuse bands at 705, 707, 713 and 719 nm was observed at 1001 °C one would expect that even at higher temperatures this excimer emission might be used to test stimulated emission which would eventually lead to the first clear observation of the alkali excimer transition laser [22, 23]. In the present experimental condition of the superheated cesium vapor the absorption coefficient at diffuse band peaks will remain constant, whereas the emission will gradually increase, thus enabling enhanced excimer emission at 705, 707, 713 and 719 nm. Inserting such cell with superheated cesium vapor within appropriate cavity an excimer laser emission might be expected.

All-sapphire cells [24] and nickel heat-pipe ovens [25] could be fabricated to stand temperatures even above 1000 °C. These high temperature cells are of great importance

for the thermionic solar converters using cesium vapor in order to diminish the negative effect of the space charge [26–28]. For the modeling of those devices it will be of considerable importance to take into account the self-emission of high temperature cesium vapor in which the amount of stable cesium dimers is almost negligible. However, the formation of the excited states of cesium dimer and the corresponding excimer emission through the triplet state manifold should be taken into account. Another type of the solar converters use PETE (photon-enhanced thermionic emission) effect where the cathode is made of semiconductor material and is illuminated by solar photons above the band gap [29, 30]. In PETE devices cesium is added between the electrodes, at low vapor pressures, for the same reason of partial space charge degradation, and the question of molecular role may arise at higher temperatures.

5. Conclusion

We measured thermal emission from the superheated cesium vapor at very high temperatures from 700 °C to 1000 °C. This was performed in the condition of no liquid cesium presence in the all-sapphire cell. We observed a number of atomic and molecular spectral features in emission and absorption, in particular a peculiar thermal emission of cesium dimer diffuse bands (Cs_2 2 $^3\Pi_g \rightarrow$ a $^3\Sigma_u^+$ transitions) at 705, 707, 713 and 719 nm which coexisted with absorption bands around first resonance lines at 852 and 894 nm. We performed appropriate calculations of the diffuse band emission profiles and compared them with observed emission profiles. Hot cesium vapor could be used for the energy conversion devices. It is therefore of interest to investigate the intrinsic emission of cesium vapor in the temperature interval from 700 °C to 1000 °C and higher. The application of the observed phenomena to the solar energy conversion will be studied in the near future.

References

[1] Vadla C, Horvatic V and Niemax K 2006 *Appl. Phys.* B **84** 523–7
[2] Vadla C, Beuc R, Horvatic V, Movre M, Quentmeier A and Niemax K 2006 *Eur. Phys. J.* D **37** 37–49

[3] Vdović S, Sarkisyan D and Pichler G 2006 *Opt. Commun.* **268** 58–63

[4] Aumiler D, Ban T and Pichler G 2005 *Phys. Rev.* A **71** 063803–6

[5] Pichler G, Makdisi Y, Kokaj J, Thomas N and Mathew J 2015 *J. Phys. B: At. Mol. Opt. Phys.* **48** 165002–8

[6] Ban T, Skenderović H, Ter-Avetisyan S and Pichler G 2001 *App. Phys.* B **72** 337–41

[7] Pichler G, Milosevic S, Veza D and Beuc R 1983 *J. Phys. B: At. Mol. Phys.* **16** 4619–31

[8] Dion C M, Dulieu O, Comparat D, de Souza Melo W, Vanhaecke N, Pillet P, Beuc R, Milosevic S and Pichler G 2002 *Eur. Phys. J. D* **18** 365–70

[9] Niemax K 1977 *J. Quant. Spectrosc. Radiat. Transfer* **17** 747–50

[10] Arp U, Vest R, Houston J and Lucatorto T 2014 *Appl. Optics* **53** 1089–93

[11] Taylor J B and Langmuir I 1937 *Phys. Rev.* **51** 753–60

[12] Nesmeyanov A N 1963 *Vapor Pressure of the Chemical Elements* (Amsterdam/London, New York: Elsevier) p 445

[13] Sarkisyan D H, Sarkisyan A S and Yalanusyan A K 1998 *Appl. Phys.* B **66** 241–4

[14] Veza D, Beuc R, Milosevic S and Pichler G 1998 *Eur. Phys. J. D* **2** 45–52

[15] Beuc R, Skenderović H, Ban T, Veža D, Pichler G and Meyer W 2001 *Eur. Phys. J. D* **15** 209–14

[16] Spies N 1989 *PhD Thesis* University of Keiserslautern

[17] Beuc R, Movre M and Horvatić B 2014 *Eur. Phys. J. D* **68** 59–8

[18] Colbert D T and Miller W H 1992 *J. Chem. Phys.* **96** 1982–91

[19] Horvatić B, Beuc R and Movre M 2015 *Eur. Phys. J. D* **69** 113–5

[20] Moroshkin P, Weller L, Saß A, JKlaers J and Weitz M 2014 *Phys. Rev. Lett.* **113** 063002–5

[21] Thorne A., Litzen U. and Johansson S. 1999 *Spectrophysics, Principles and Applications* (Berlin: Springer)

[22] Bahns J T and Stwalley W C 1984 *Appl. Phys. Lett.* **44** 826

[23] Schlejen J, Jalink C J and Woerdman J P 1987 *Optics. Comm.* **64** 131–6

[24] Glushko B, Kryzhanovsky B and Sarkisyan D 1993 *Phys. Rev. Lett.* **71** 243–6

[25] Pichler G and Carlsten J L 1978 *J. Phys. B: At. Mol. Phys.* **11** L483–8

[26] Ogino A, Muramatsu T and Kando M 2004 *Japan. J. Appl. Phys.* **43** 309–14

[27] Inaguma T, Tsuda N and Yamada J 2007 *Electr. Eng. Japan* **158** 14–21

[28] Vadla C, Horvatic V, Veza D and Niemax K 2010 *Spectrochim. Acta Part* B **65** 33–45

[29] Schwede J W *et al* 2010 *Nat. Mater.* **9** 762–7

[30] Segev G, Rosenwaks Y and Kribus A 2015 *Sol. Energy Mater. Sol. Cells* **140** 464–76